Ultrafast State Preparation via the Quantum Approximate Optimization Algorithm with Long Range Interactions

Wen Wei Ho,[1] Cheryne Jonay,[2] and Timothy H. Hsieh[2]

[1] *Department of Physics, Harvard University, Cambridge, Massachusetts 02138, USA*
[2] *Perimeter Institute for Theoretical Physics, Waterloo, Ontario N2L 2Y5, Canada*

(Dated: October 12, 2018)

State preparation protocols ideally require as minimal a circuit depth as possible, in order to be implemented in near-term quantum devices. Motivated by long range interactions (LRI) intrinsic to many experimental platforms (trapped ions, Rydberg atom arrays, etc.), we investigate the performance of the quantum approximate optimization algorithm (QAOA) with LRIs for the preparation of non-trivial quantum states. We show that this approach leads to extremely efficient state preparation: for example, Greene-Horne-Zeilinger (GHZ) states can be prepared with $O(1)$ circuit depth, and a quantum critical point of the long range transverse field Ising model (TFIM) can be prepared with $> 99\%$ fidelity on a 100 qubit system with *only one* iteration of QAOA. Furthermore, we show that QAOA with LRIs is a promising route for exploring generic points in the phase diagram of the long-range TFIM. Our approach thus provides concrete, ultrafast protocols for quantum simulators equipped with long range interactions.

arXiv:1810.04817v1 [cond-mat.str-el] 11 Oct 2018

Rapid experimental progress in the precise control of synthetic quantum systems, like trapped ions [1–3], ultracold atoms [4–6] and superconducting qubits [7, 8], has unlocked the potential for quantum computation and simulation [8, 9], quantum sensing and metrology [10–13], and also the simulation of quantum many-body phases of matter [4, 14–21]. These tasks require the ability to create, with good fidelity, quantum states containing nontrivial entanglement such as Greene-Horne-Zeilinger (GHZ) states and topologically ordered states. A central challenge is therefore finding efficient state preparation protocols: ideally, these protocols should have as minimal a circuit depth as possible to be realistically implemented in such quantum simulators, in order to suppress the errors that accumulate during runtime.

Recently, the quantum approximate optimization algorithm (QAOA) has emerged as one such promising candidate for a quantum state preparation protocol [22, 23]. In short, the QAOA is a hybrid quantum-classical bang-bang protocol that specifically incorporates feedback: it takes as an input a set of angles that specifies the durations for which time evolution between two different Hamiltonians is alternated between, in the quantum simulator. Then, measurements are performed and the subsequent optimization of a cost function (e.g. energy, by means of a classical computer) yields a new set of angles which is fed back into the simulator. Such QAOA-type circuits, with spatially local Hamiltonians, have been shown to be able to transform trivial product states into GHZ, quantum critical, and topologically ordered states, with perfect fidelity and circuit depths scaling as $O(N)$ where N is the system's linear dimension [24]. Conceptually, the QAOA is an example of a "shortcut to adiabaticity", a direction in quantum state control that is actively being researched [25–29], as its operating principle is fundamentally different from conventional adiabatic preparation schemes [30–35].

While a circuit depth scaling as $O(N)$ is efficient from a theoretical standpoint – there exist fundamental speed limitations imposed by Lieb-Robinson bounds [36–39] constraining QAOA-circuits utilizing spatially local Hamiltonians, it still presents challenges experimentally, especially in terms of scalability to a large number of qubits. This motivates the search for alternative ultrafast, or extremely low-depth, circuits. A natural way to overcome these speed limitations is to utilize long-range interactions (LRI): in principle, even finite-depth circuits can prepare long-range correlated states, as entanglement and correlations can be built up between distant parts of the system in finite time [40–42]. Moreover, LRIs are naturally present in various experimental quantum simulator platforms, e.g. trapped ion systems (Coulomb interactions), Rydberg atom arrays (van der Waals interactions), etc., and are hence a readily accessible resource [2, 6, 43].

To this end, in this work we explore how efficiently the QAOA protocol with long range interactions can prepare non-trivial quantum states. Specifically, we consider quantum simulators that realize long-range $\sim 1/r^\alpha$ Ising interactions with tuneable range α, motivated by trapped ion experimental setups. We find that the QAOA protocol with LRIs can prepare GHZ and quantum critical states with $O(1)$ depth. In particular, in the limit of extremely long-range interactions $\alpha \to 0$, the GHZ state can be prepared with only one (two) iteration of QAOA for odd (even) system sizes. Furthermore, the quantum critical point of the Lipkin-Meshkov-Glick model [44] can be prepared with very high fidelity and low circuit depth (e.g. fidelity > 0.99 for 100 spins after one iteration). We also analyze how efficiently QAOA with long but finite range interactions can prepare points within the phase diagram of the long-range transverse field Ising model. Our results thus demonstrate the utility of extremely low depth QAOA-protocols with LRIs for near-term quan-

tum simulators to realize nontrivial many-body states of interest.

QAOA-type protocol. — We quickly recapitulate the QAOA [22, 23], which we modify for our purposes. Our aim is to prepare a target state $|\psi_t\rangle$ with as high fidelity as possible. Usually, $|\psi_t\rangle$ will be taken to be the ground state of a certain Hamiltonian, called the target Hamiltonian H_t.

The QAOA starts off with an easily prepared initial state such as an unentangled product state, for example the ground state $|+\rangle$ of a simple, paramagnetic Hamiltonian $H_X = -\sum_i X_i$, which we will take from here on out. One then time evolves in an alternating fashion between H_X and an "interaction Hamiltonian" denoted H_I for a total of p pairs of times:

$$|\psi(\vec{\gamma},\vec{\beta})\rangle_p = e^{-i\beta_p H_X} e^{-i\gamma_p H_I} \cdots e^{-i\beta_1 H_X} e^{-i\gamma_1 H_I} |+\rangle, \quad (1)$$

with evolution times given by the angles $(\vec{\gamma},\vec{\beta}) \equiv (\gamma_1, \cdots \gamma_p, \beta_1, \beta_p)$ respectively. We label this protocol as QAOA_p; it has a circuit depth $2p$.

As the goal is to closely approximate the ground state of H_t, one can seek to find the evolution times $(\vec{\gamma},\vec{\beta})$ which minimize a given cost function $F_p(\vec{\gamma},\vec{\beta})$, usually taken to be the energy with respect to H_t:

$$F_p(\vec{\gamma},\vec{\beta}) = {}_p\langle\psi(\vec{\gamma},\vec{\beta})|H_t|\psi(\vec{\gamma},\vec{\beta})\rangle_p. \quad (2)$$

As can be easily seen, increasing the circuit depth p of the QAOA circuit can only improve the minimal value F_p^*, i.e. $F_{p+1}^* \leq F_p^*$.

In practice, such a protocol can be implemented in a hybrid setup involving a quantum simulator and a classical computer: one first feeds the quantum simulator an initial seed of angles, which produces a certain state $|\psi(\vec{\gamma},\vec{\beta})\rangle$. Then, leveraging upon single-site accesibility in near-term quantum platforms, one measures correlations within the state and determines the cost function (2), e.g. the global energy. A classical computer is then used to obtain the next set of angles $(\vec{\gamma},\vec{\beta})$ to be fed into the quantum simulator, by means of an optimization algorithm such as gradient descent or a similar protocol. The entire process is then repeated until either the global minimum F_p^* is found, or a desired energy/fidelity threshold is attained.

The choice of interaction Hamiltonian H_I is motivated by the structure of the target Hamiltonian H_t. For example, consider targeting the ground state of the one-dimensional transverse field Ising model (TFIM) with nearest neighbor interactions:

$$H_{TFIM} = -\sum_{i=1}^{N} Z_i Z_{i+1} - h\sum_{i=1}^{N} X_i, \quad (3)$$

where h parameterizes the field strength and N is the number of qubits. Given this target Hamiltonian, a natural choice for the interaction Hamiltonian is thus $H_I = -\sum_{i=1}^{N} Z_i Z_{i+1}$. In this case, the QAOA protocol is guaranteed to work in the limit of $p \to \infty$ for any finite size system (there always exists a finite gap), as an asymptotically slow adiabatic preparation scheme can always be trotterized to the form (1). However, non-trivial behavior and an improvement over adiabaticity can arise for small p, the regime of validity for experimental systems. Indeed, in a previous work, it was shown that in this specific example, the resulting protocol at depth N ($\text{QAOA}_{N/2}$), can target with *perfect fidelity* the ground state of the model at $h = 0, 1$ (GHZ and quantum critical state, respectively) [24]. It was further conjectured and supported with numerical evidence that this result generalizes to all points in the phase diagram of the model.

QAOA with LRIs. — Despite impressive progress in improving the fidelity of single qubit and two qubit gates, near-term synthetic quantum systems nevertheless have a lack of fault tolerance, and so they are prone to increasing errors with increasing circuit depth. Thus, even a circuit depth scaling as $O(N)$ poses challenges to scalability to large number of qubits in such platforms. Fundamentally, such scaling is dictated by speed limits due to information propagation bounds (specifically, Lieb-Robinson bounds) in systems with local interactions – in short, in order for the pattern of correlations in a quantum state to change dramatically, spatially distant parts of the system must get entangled; however, local interactions give rise to a linear light cone $r \sim vt$ of information propagation, and so the time taken in a finite system of size N must be at least $t \geq O(N)$.

Long-range interactions (LRIs) have less stringent speed limits [42] and can thus dramatically speed up state preparation protocols. We now show that QAOA with LRIs is a viable method for efficiently targeting nontrivial quantum states.

Specifically, consider quantum simulators where long-range Ising interactions (with power-law interactions $\sim 1/r^\alpha$) can be realized, such as trapped ions experiments. Together with a readily applicable transverse field, effective Hamiltonians of the form

$$H = -\sum_{i<j}^{N} J_{ij} Z_i Z_j - \mathcal{N} h \sum_{i}^{N} X_i \quad (4)$$

can be created in these setups, where $J_{ij} = \frac{J_0}{|i-j|^\alpha}$ and α can vary in principle between 0 and 3. We have chosen the normalization of (4) such that $J_0 = 1$ and $\mathcal{N} = \frac{1}{N-1}\sum_{i<j} J_{ij}$. Note that with this choice, the $\alpha \to \infty$ regime reduces to the nearest neighbor TFIM model with open boundary conditions.

In the following, we will analyze the small α regime of the Hamiltonian (4) and show that low, $O(1)$ depth QAOA circuits are sufficient to prepare its ground states. Given the structure of the Hamiltonian, it is thus natural

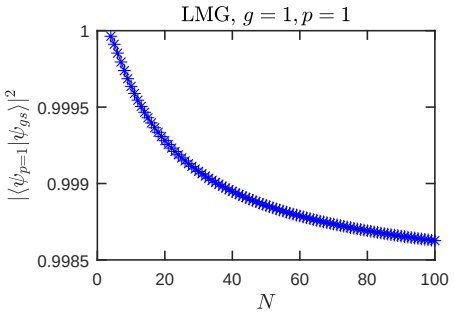

Figure 1. Fidelity $|\langle\psi_{QCP}|\psi(\vec{\gamma},\vec{\beta})\rangle_{p=1}|^2$ in preparation of LMG critical state as a function of system size N, for QAOA depth $p = 1$. Remarkably, even at $N = 100$, the fidelity is very close to unity ($> 99\%$).

to choose for the QAOA protocol

$$H_I = -\sum_{i<j} J_{ij} Z_i Z_j, \quad H_X = -\sum_i X_i. \tag{5}$$

We will restrict the QAOA parameter space to $\gamma \in [-\pi, \pi)$ and $\beta \in [0, \pi/2)$. The former is motivated by experimental limitations on the evolution time, and the latter is because $e^{-i(\pi/2)H_X} \propto \prod_i X_i$ which is conserved throughout the evolution.

GHZ & quantum critical state preparation in the Lipkin-Meshkov-Glick model, $\alpha = 0$. — We first consider the case $\alpha = 0$ of (4), in which the N qubits interact in an all-to-all fashion. Then, up to an overall multiplicative factor and also an inconsequential shift in energy, (4) can be seen to be equivalent to the Lipkin-Meshkov-Glick (LMG) model

$$H_{LMG} = -\frac{2}{N} S_z^2 - 2gS_x, \tag{6}$$

where the total spin operators are $S_z = \sum_i^N Z_i/2$ and $S_x = \sum_i^N X_i/2$, and $g = h/2$. As is the case with the nearest-neighbor TFIM model, the ground states are ferromagnetic GHZ states at $g = 0$, and a quantum phase transition at $g = 1$ separates the ferromagnet from the paramagnetic phase.

We now show that a $p = 1$ QAOA circuit suffices to produce the ground state of (6) at $g = 0$, i.e. the GHZ state, for odd system size N. To see this, we explicitly derive the energy cost function (2) for the LMG model with $\text{QAOA}_{p=1}$, which yields:

$$\begin{aligned} F_{p=1}(\gamma,\beta) = -\frac{N-1}{4}\Big(&\sin(2\beta)^2(1-\cos(4\gamma)^{N-2}) \\ &+2\sin(4\beta)\sin(2\gamma)\cos(2\gamma)^{N-2}\Big) \\ &-gN\cos(2\gamma)^{N-1} - 1/2 \end{aligned} \tag{7}$$

(see [45] for the derivation). From the above, it is evident that for odd N, the ground state energy of $H_{LMG}|_{g=0}$, namely $E_0 = -N/2$, can be achieved with the angles $(\gamma,\beta) = (\pi/4, \pi/4)$. Thus, in such cases, we see that the ferromagnetic GHZ state, a state with macroscopic superposition of entanglement $(1/\sqrt{2})(|0...0\rangle + |1...1\rangle)$, can be created with two operations:

$$|GHZ\rangle = e^{-i(\pi/4)H_X} e^{-i(\pi/4)H_I} |+\rangle. \tag{8}$$

We note that there exist various preparation schemes that create macroscopic GHZ states, one of which is the Molmer-Sorenson (MS) protocol involving time evolution with S_x^2 [46, 47]. Although the QAOA protocol discussed above resembles the MS protocol, there are several differences: MS begins with the (Ising symmetry broken) ground state $|0...0\rangle$ and prepares a GHZ state whose relative phase between the cat states depends on system size. In contrast, since the Ising symmetry $\prod_i X_i$ is always conserved during the implementation of the QAOA protocol and since we begin with the symmetric state $|+\rangle$, the end result is that we will always prepare the symmetric GHZ state, independent of system size.

The distinction between MS and our protocol is most manifest for even system sizes, in which we find that the GHZ state is instead achieved with perfect fidelity with a $p = 2$ QAOA protocol:

$$|GHZ\rangle = e^{-i(\pi/4)H_X} e^{-i(\pi/8)H_I} e^{-i(3\pi/4N)H_X} e^{-i(\pi/4)H_I} |+\rangle.$$

Note that from (7), there is no range of parameters that give perfect fidelity for $p = 1$ for even N. We show in the appendix [45] the derivation of the above result. These results already demonstrate the utility of LRIs with QAOA: they enable an ultrashort, $O(1)$ depth circuit to prepare with perfect fidelity a macroscopic GHZ state.

Besides the GHZ state, we find that the QAOA approach with LRIs is general and can target many other interesting states. One state of particular interest is the quantum critical point of the LMG model at $g = 1$ and is a highly correlated state $|\psi_{QCP}\rangle$. By numerically optimizing for the energy of (6) at $g = 1$, we find that the QAOA protocol with only $p = 1$ is already sufficient to achieve the critical state with extremely high fidelity $|\langle\psi_{QCP}|\psi(\vec{\gamma},\vec{\beta})\rangle_{p=1}|^2$, even for very large system sizes ($> 99\%$ at ~ 100 qubits) (see Fig. 1). This is a remarkably efficient protocol for preparing a quantum critical state.

Note that the gap at the critical point of the LMG model scales as $\Delta \propto N^{-1/3}$ [44], and thus the adiabatic algorithm requires $O(N^{1/3})$ time to prepare the GHZ and critical states. However, in order to make a direct comparison with the adiabatic algorithm, we would need to scale down the exchange interaction in Eq. 5 by N, and thus the total preparation time in this convention would scale with N. Our intention is not to make this theoretical comparison, but instead to make contact with existing experiments. In recent experiments,

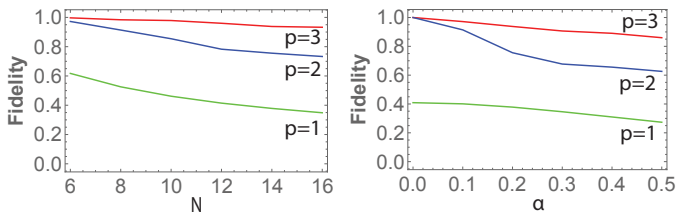

Figure 2. (Left) Fidelity in preparation of GHZ state as a function of system size N, for $\alpha = 0.2$. One sees that with increasing N, the fidelity decreases. However, this can be compensated by going to higher ps. (Right) Fidelity in preparation of GHZ state as a function of α, for $N = 14$. One sees that generically, interactions that are longer-range (smaller α) are more helpful in targeting the desired state.

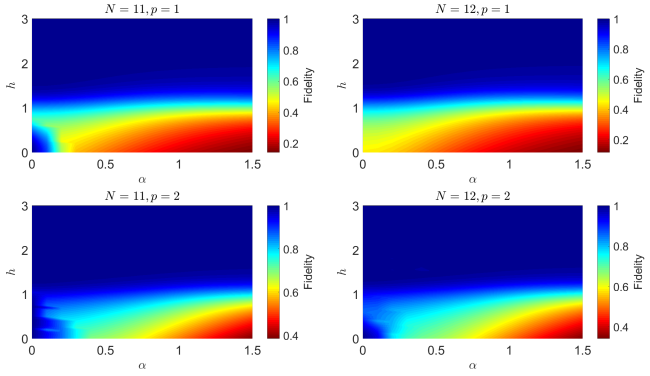

Figure 3. Heat map depicting fidelities in the state preparation of the ground state of the long-range TFIM (3) for system sizes $N = 11$, and for 12, $p = 1, 2$. Blue (red) regions demarcate regions of high (low) fidelity. As noted before, there is an odd-even system size distinction near $\alpha \approx 0$, $h \approx 0$ for $p = 1$, but this distinction vanishes at the next level, $p = 2$.

the nearest-neighbor exchange interaction J_0 does not necessarily decrease with system size; for example, it is $(0.82, 0.56, 0.38, 0.65)kHz$ for $N = (8, 12, 16, 53)$ respectively [2]. Hence, the interactions in Eq. 5 are reasonable in near-term trapped ion experiments and lead to $O(1)$ preparation time for the GHZ and critical states. The simplicity and discreteness of the protocols we have presented may offer advantages over the adiabatic algorithm with or without counter-diabatic terms [29, 48–50].

GHZ preparation with finite α. – In practice, there may be challenges in realizing strictly all-to-all ($\alpha = 0$) Ising interactions, and therefore we analyze how well the finite α QAOA protocol can prepare the GHZ state.

In the left panel of Fig. 2, we fix $\alpha = 0.2$ and show the fidelity with GHZ state achieved for $\text{QAOA}_{p=1,2,3}$ for even system sizes. As expected, $\text{QAOA}_{p=2}$ no longer prepares the state with perfect fidelity unlike the $\alpha = 0$ case (for any system size), but this can be addressed with further iterations of QAOA (note the high fidelities achieved by $p = 3$ for system sizes up to $N = 16$). The long-range interactions establish correlations between spins separated by a distance r in time $O(r^\alpha)$, which surpasses the light cone bound for local interactions [40–42]. Hence, we expect that the depth required to prepare the state with some fixed error in fidelity scales as $O(N^{\alpha'}), \alpha' < 1$. Also plotted is the optimal fidelity for different values of α and for fixed system size $N = 14$. These results indicate that longer interaction range (smaller α) yield higher fidelities, and errors can be effectively reduced using further QAOA iterations [51].

Exploring the phase diagram of the long-range TFIM. — Finally, we explore how well the QAOA protocol can prepare the ground states at generic points in the phase diagram of the long-range TFIM model (4). Plotted in Fig. 3 are the fidelities as a function of transverse field h and interaction range α, for $N = 11, 12$ and for $p = 1, 2$.

It is known that the long-range TFIM (3) supports a ferromagnetic-paramagnetic ground state quantum phase transition for each value of α, upon tuning h. In the limits $\alpha \to 0$, the critical magnetic field $h_c = 2$, while in the limit $\alpha \to \infty$, the critical magnetic field $h_c = 1$. For intermediate values of α, previous works have attempted to map out how h_c varies (see e.g. [52, 53] and [54, 55] for the antiferromagnetic model). As expected, from Fig. 3, at the system sizes considered, the QAOA with LRIs is able to target ground states within the paramagnetic phase (large h) relatively easily, while for the ferromagnetic phase (small h) it becomes more difficult to prepare as the interactions become more short-ranged (larger α). Note that for larger α, the region where state preparation is difficult (red region) is separated from the region where state preparation is easy (blue region) near the value $h \approx 1$, which agrees with the critical points h_c of the nearest-neighbor TFIM, which is realized in the asymptotic limit $\alpha \to \infty$.

As the small α regime of this model is somewhat challenging for numerical studies [52], it serves as a venue in which the quantum-classical hybrid implementation of QAOA could provide valuable input. Moreover, the small α window is precisely the regime in which the QAOA approach requires only short-depth circuits.

Discussion and conclusion. — We have shown that QAOA-type protocols with long-range interactions allow for ultra-fast state preparation. In particular, the Ising-symmetric GHZ state can be prepared exactly at finite depth $p = 1(2)$ for odd (even) system sizes. We have also demonstrated that other states of interest, for example the quantum critical point of the Lipkin-Meshkov-Glick model, can also be prepared very efficiently. QAOA with long range interactions thus provides an opportunity for near-term simulators to prepare non-trivial states with very high fidelity and to shed light on areas of phase diagrams that are challenging for numerics.

Note added: While completing this manuscript, we became aware of related works [56] and [57].

Acknowledgments. – We thank R. Islam, C. Monroe, and B. Yoshida for useful discussions. WWH is supported by the Gordon and Betty Moore Foundations EPiQS Initiative through Grant No. GBMF4306. Research at Perimeter Institute is supported by the Government of Canada through Industry Canada and by the Province of Ontario through the Ministry of Research and Innovation. This work was performed in part at the Aspen Center for Physics, which is supported by National Science Foundation grant PHY-1607611.

[1] R. Blatt and C. F. Roos, "Quantum simulations with trapped ions," Nature Physics **8**, 277–284 (2012).

[2] J. Zhang, G. Pagano, P. W. Hess, A. Kyprianidis, P. Becker, H. Kaplan, A. V. Gorshkov, Z.-X. Gong, and C. Monroe, "Observation of a many-body dynamical phase transition with a 53-qubit quantum simulator," Nature **551**, 601 EP – (2017).

[3] R. Islam, C. Senko, W. C. Campbell, S. Korenblit, J. Smith, A. Lee, E. E. Edwards, C.-C. J. Wang, J. K. Freericks, and C. Monroe, "Emergence and frustration of magnetism with variable-range interactions in a quantum simulator," Science **340**, 583–587 (2013).

[4] Markus Greiner, Olaf Mandel, Tilman Esslinger, Theodor W. Hänsch, and Immanuel Bloch, "Quantum phase transition from a superfluid to a mott insulator in a gas of ultracold atoms," Nature **415**, 39 EP – (2002), article.

[5] Immanuel Bloch, Jean Dalibard, and Wilhelm Zwerger, "Many-body physics with ultracold gases," Rev. Mod. Phys. **80**, 885–964 (2008).

[6] Hannes Bernien, Sylvain Schwartz, Alexander Keesling, Harry Levine, Ahmed Omran, Hannes Pichler, Soonwon Choi, Alexander S. Zibrov, Manuel Endres, Markus Greiner, Vladan Vuletic, and Mikhail D. Lukin, "Probing many-body dynamics on a 51-atom quantum simulator," Nature **551**, 579 EP – (2017), article.

[7] M. H. Devoret and R. J. Schoelkopf, "Superconducting circuits for quantum information: an outlook," Science **339**, 1169 (2013).

[8] Jay M. Gambetta, Jerry M. Chow, and Matthias Steffen, "Building logical qubits in a superconducting quantum computing system," npj Quantum Information **3**, 2 (2017).

[9] Michael Schreiber, Sean S. Hodgman, Pranjal Bordia, Henrik P. Lüschen, Mark H. Fischer, Ronen Vosk, Ehud Altman, Ulrich Schneider, and Immanuel Bloch, "Observation of many-body localization of interacting fermions in a quasirandom optical lattice," Science **349**, 842–845 (2015).

[10] D. Leibfried, M. D. Barrett, T. Schaetz, J. Britton, J. Chiaverini, W. M. Itano, J. D. Jost, C. Langer, and D. J. Wineland, "Toward heisenberg-limited spectroscopy with multiparticle entangled states," Science **304**, 1476–1478 (2004).

[11] Vittorio Giovannetti, Seth Lloyd, and Lorenzo Maccone, "Quantum-enhanced measurements: Beating the standard quantum limit," Science **306**, 1330–1336 (2004).

[12] C. L. Degen, F. Reinhard, and P. Cappellaro, "Quantum sensing," Rev. Mod. Phys. **89**, 035002 (2017).

[13] S. Choi, N. Y. Yao, and M. D. Lukin, "Quantum metrology based on strongly correlated matter," ArXiv e-prints (2018), arXiv:1801.00042 [quant-ph].

[14] M. Aidelsburger, M. Atala, M. Lohse, J. T. Barreiro, B. Paredes, and I. Bloch, "Realization of the hofstadter hamiltonian with ultracold atoms in optical lattices," Phys. Rev. Lett. **111**, 185301 (2013).

[15] M. Aidelsburger, M. Lohse, C. Schweizer, M. Atala, J.T. Barreiro, S. Nascimbène, N. R. Cooper, I. Bloch, and N. Goldman, "Measuring the chern number of hofstadter bands with ultracold bosonic atoms," Nature Physics **11**, 162 EP – (2014).

[16] Rajibul Islam, Ruichao Ma, Philipp M. Preiss, M. Eric Tai, Alexander Lukin, Matthew Rispoli, and Markus Greiner, "Measuring entanglement entropy in a quantum many-body system," Nature **528**, 77 EP – (2015), article.

[17] Jae-yoon Choi, Sebastian Hild, Johannes Zeiher, Peter Schauß, Antonio Rubio-Abadal, Tarik Yefsah, Vedika Khemani, David A. Huse, Immanuel Bloch, and Christian Gross, "Exploring the many-body localization transition in two dimensions," Science **352**, 1547–1552 (2016).

[18] J. Smith, A. Lee, P. Richerme, B. Neyenhuis, P. W. Hess, P. Hauke, M. Heyl, D. A. Huse, and C. Monroe, "Many-body localization in a quantum simulator with programmable random disorder," Nature Physics **12**, 907 EP – (2016).

[19] Soonwon Choi, Joonhee Choi, Renate Landig, Georg Kucsko, Hengyun Zhou, Junichi Isoya, Fedor Jelezko, Shinobu Onoda, Hitoshi Sumiya, Vedika Khemani, Curt von Keyserlingk, Norman Y. Yao, Eugene Demler, and Mikhail D. Lukin, "Observation of discrete time-crystalline order in a disordered dipolar many-body system," Nature **543**, 221–225 (2017).

[20] J. Zhang, P. W. Hess, A. Kyprianidis, P. Becker, A. Lee, J. Smith, G. Pagano, I.-D. Potirniche, A. C. Potter, A. Vishwanath, N. Y. Yao, and C. Monroe, "Observation of a discrete time crystal," Nature **543**, 217–220 (2017).

[21] J. Choi, H. Zhou, S. Choi, R. Landig, W. W. Ho, J. Isoya, F. Jelezko, S. Onoda, H. Sumiya, D. A. Abanin, and M. D. Lukin, "Probing quantum thermalization of a disordered dipolar spin ensemble with discrete time-crystalline order," ArXiv e-prints (2018), arXiv:1806.10169 [quant-ph].

[22] E. Farhi, J. Goldstone, and S. Gutmann, "A Quantum Approximate Optimization Algorithm," ArXiv e-prints (2014), arXiv:1411.4028 [quant-ph].

[23] E. Farhi and A. W Harrow, "Quantum Supremacy through the Quantum Approximate Optimization Algorithm," ArXiv e-prints (2016), arXiv:1602.07674 [quant-ph].

[24] W. W. Ho and T. H. Hsieh, "Efficient unitary preparation of non-trivial quantum states," ArXiv e-prints (2018), arXiv:1803.00026 [cond-mat.str-el].

[25] Mustafa Demirplak and Stuart A. Rice, "Adiabatic population transfer with control fields," The Journal of Physical Chemistry A **107**, 9937–9945 (2003), https://doi.org/10.1021/jp030708a.

[26] Mustafa Demirplak and Stuart A. Rice, "Assisted adi-

abatic passage revisited," The Journal of Physical Chemistry B **109**, 6838–6844 (2005), pMID: 16851769, https://doi.org/10.1021/jp040647w.
[27] M V Berry, "Transitionless quantum driving," Journal of Physics A: Mathematical and Theoretical **42**, 365303 (2009).
[28] K. Agarwal, R. N. Bhatt, and S. L. Sondhi, "Fast preparation of critical ground states using superluminal fronts," ArXiv e-prints (2017), arXiv:1710.09840 [cond-mat.quant-gas].
[29] Dries Sels and Anatoli Polkovnikov, "Minimizing irreversible losses in quantum systems by local counterdiabatic driving," Proceedings of the National Academy of Sciences (2017), 10.1073/pnas.1619826114.
[30] E. Farhi, J. Goldstone, S. Gutmann, and M. Sipser, "Quantum Computation by Adiabatic Evolution," eprint arXiv:quant-ph/0001106 (2000), quant-ph/0001106.
[31] Edward Farhi, Jeffrey Goldstone, Sam Gutmann, Joshua Lapan, Andrew Lundgren, and Daniel Preda, "A quantum adiabatic evolution algorithm applied to random instances of an np-complete problem," Science **292**, 472–475 (2001).
[32] L.S. Pontryagin, *Mathematical Theory of Optimal Processes* (1987).
[33] Robert F. Stengel, *Optimal Control and Estimation* (1994).
[34] Constantin Brif, Matthew D Grace, Mohan Sarovar, and Kevin C Young, "Exploring adiabatic quantum trajectories via optimal control," New Journal of Physics **16**, 065013 (2014).
[35] Zhi-Cheng Yang, Armin Rahmani, Alireza Shabani, Hartmut Neven, and Claudio Chamon, "Optimizing variational quantum algorithms using pontryagin's minimum principle," Phys. Rev. X **7**, 021027 (2017).
[36] Elliott H. Lieb and Derek W. Robinson, "The finite group velocity of quantum spin systems," Comm. Math. Phys. **28**, 251–257 (1972).
[37] Michael A. Nielsen, "A geometric approach to quantum circuit lower bounds," Quantum Info. Comput. **6**, 213–262 (2006).
[38] S. Bravyi, M. B. Hastings, and F. Verstraete, "Lieb-robinson bounds and the generation of correlations and topological quantum order," Phys. Rev. Lett. **97**, 050401 (2006).
[39] M. B. Hastings, "Locality in Quantum Systems," ArXiv e-prints (2010), arXiv:1008.5137 [math-ph].
[40] Takuro Matsuta, Tohru Koma, and Shu Nakamura, "Improving the lieb–robinson bound for long-range interactions," Annales Henri Poincaré **18**, 519–528 (2017).
[41] Michael Foss-Feig, Zhe-Xuan Gong, Charles W. Clark, and Alexey V. Gorshkov, "Nearly linear light cones in long-range interacting quantum systems," Phys. Rev. Lett. **114**, 157201 (2015).
[42] M. C. Tran, A. Y. Guo, Y. Su, J. R. Garrison, Z. Eldredge, M. Foss-Feig, A. M. Childs, and A. V. Gorshkov, "Locality and digital quantum simulation of power-law interactions," ArXiv e-prints (2018), arXiv:1808.05225 [quant-ph].
[43] Philip Richerme, Zhe-Xuan Gong, Aaron Lee, Crystal Senko, Jacob Smith, Michael Foss-Feig, Spyridon Michalakis, Alexey V. Gorshkov, and Christopher Monroe, "Non-local propagation of correlations in quantum systems with long-range interactions," Nature **511**, 198 EP – (2014).
[44] H.J. Lipkin, N. Meshkov, and A.J. Glick, "Validity of many-body approximation methods for a solvable model: (i). exact solutions and perturbation theory," Nuclear Physics **62**, 188 – 198 (1965).
[45] Supplemental material online.
[46] Anders Sørensen and Klaus Mølmer, "Entanglement and quantum computation with ions in thermal motion," Phys. Rev. A **62**, 022311 (2000).
[47] Thomas Monz, Philipp Schindler, Julio T. Barreiro, Michael Chwalla, Daniel Nigg, William A. Coish, Maximilian Harlander, Wolfgang Hänsel, Markus Hennrich, and Rainer Blatt, "14-qubit entanglement: Creation and coherence," Phys. Rev. Lett. **106**, 130506 (2011).
[48] Adolfo del Campo, "Shortcuts to adiabaticity by counterdiabatic driving," Phys. Rev. Lett. **111**, 100502 (2013).
[49] Steve Campbell, Gabriele De Chiara, Mauro Paternostro, G. Massimo Palma, and Rosario Fazio, "Shortcut to adiabaticity in the lipkin-meshkov-glick model," Phys. Rev. Lett. **114**, 177206 (2015).
[50] Steve Campbell and Sebastian Deffner, "Trade-off between speed and cost in shortcuts to adiabaticity," Phys. Rev. Lett. **118**, 100601 (2017).
[51] We note that the numerical optimization in our simulations may output local minima in the cost function, and thus the results presented in Fig. 2 are lower bounds on the optimal fidelities.
[52] Daniel Jaschke, Kenji Maeda, Joseph D Whalen, Michael L Wall, and Lincoln D Carr, "Critical phenomena and kibblezurek scaling in the long-range quantum ising chain," New Journal of Physics **19**, 033032 (2017).
[53] Sebastian Fey and Kai Phillip Schmidt, "Critical behavior of quantum magnets with long-range interactions in the thermodynamic limit," Phys. Rev. B **94**, 075156 (2016).
[54] Thomas Koffel, M. Lewenstein, and Luca Tagliacozzo, "Entanglement entropy for the long-range ising chain in a transverse field," Phys. Rev. Lett. **109**, 267203 (2012).
[55] Davide Vodola, Luca Lepori, Elisa Ercolessi, and Guido Pupillo, "Long-range ising and kitaev models: phases, correlations and edge modes," New Journal of Physics **18**, 015001 (2016).
[56] C. Kokail, C. Maier, R. van Bijnen, T. Brydges, M. Joshi, P. Jurcevic, C. Muschik, P. Silvi, R. Blatt, C. Roos, and P. Zoller, "Self-Verifying Variational Quantum Simulation of the Lattice Schwinger Model," ArXiv e-prints (2018), arXiv:1810.03421 [quant-ph].
[57] A. Bapat et.al., In preparation (2018).

SUPPLEMENTAL INFORMATION

LMG Cost Function for $p = 1$

We evaluate

$$\langle +|e^{i\gamma H_I} e^{i\beta H_X} H_{LMG} e^{-i\beta H_X} e^{-i\gamma H_I}|+\rangle, \tag{9}$$

where

$$H_{LMG} = -\frac{2}{N} S_z^2 - 2gS_x \tag{10}$$

The second piece gives

$$-g\langle +|e^{i\gamma H_I} \sum_i X_i e^{-i\gamma H_I}|+\rangle \tag{11}$$

$$= -g\langle +| \prod_{j\neq i} (\cos(\gamma) - i\sin(\gamma) Z_i Z_j) \sum_i X_i \prod_{j\neq i} (\cos(\gamma) + i\sin(\gamma) Z_i Z_j)|+\rangle \tag{12}$$

Because any operator aside from identity and X has zero expectation value in $|+\rangle$, we get contributions only from $\cos^2(\gamma) - \sin^2(\gamma)$ for each j. In total, this piece is $(-gN)(\cos(2\gamma))^{N-1}$.

The first piece is

$$-\frac{N-1}{2}\langle +|e^{i\gamma H_I} e^{i\beta H_X} Z_i Z_j e^{-i\beta H_X} e^{-i\gamma H_I}|+\rangle - \frac{1}{2} \tag{13}$$

$$= -\frac{N-1}{2}\langle +|e^{i\gamma H_I} (\cos(2\beta) Z_i - \sin(2\beta) Y_i)(\cos(2\beta) Z_j - \sin(2\beta) Y_j) e^{-i\gamma H_I}|+\rangle - \frac{1}{2} \tag{14}$$

Again, we need only consider when the identity and X operators arise. One contribution to the matrix element comes from the evolution of $Y_i Z_j + Z_i Y_j$, which gives

$$-\sin(4\beta)\langle +| \prod_{k\neq j,i} (\cos(\gamma) - i\sin(\gamma) Z_i Z_k)(\cos(\gamma) - i\sin(\gamma) Z_i Z_j) \tag{15}$$

$$(Y_i Z_j)(\cos(\gamma) + i\sin(\gamma) Z_i Z_j) \prod_{k\neq j,i} (\cos(\gamma) + i\sin(\gamma) Z_i Z_k)|+\rangle \tag{16}$$

$$= \sin(4\beta)\sin(2\gamma)\cos(2\gamma)^{N-2} \tag{17}$$

Another contribution comes from

$$\sin(2\beta)^2\langle +| \prod_{k\neq i,j} (\cos(\gamma) - i\sin(\gamma) Z_i Z_k) \prod_{l\neq i,j} (\cos(\gamma) - i\sin(\gamma) Z_j Z_l) Y_i Y_j \tag{18}$$

$$\prod_{k\neq i,j} (\cos(\gamma) + i\sin(\gamma) Z_i Z_k) \prod_{l\neq i,j} (\cos(\gamma) + i\sin(\gamma) Z_j Z_l)|+\rangle \tag{19}$$

The transformation into two X operators requires an odd number of applications of $Z_i Z_k$ and $Z_j Z_k$; each application comes with a factor of $\sin(2\gamma)^2$. The terms which do not alter the operator come with factors of $\cos(2\gamma)^2$. Hence, to single out the odd powers, we take the combination

$$(1/2)((\cos(2\gamma)^2 + \sin(2\gamma)^2)^{N-2} - (\cos(2\gamma)^2 - \sin(2\gamma)^2)^{N-2}) \tag{20}$$

$$= (1/2)(1 - \cos(4\gamma)^{N-2}). \tag{21}$$

In total, the cost function is thus

$$-\frac{N-1}{4}(\sin(2\beta)^2(1 - \cos(4\gamma)^{N-2}) + 2\sin(4\beta)\sin(2\gamma)\cos(2\gamma)^{N-2}) - gN(\cos(2\gamma))^{N-1} - 1/2 \tag{22}$$

GHZ Preparation for Even N

We show below that for an even number N of qubits,

$$|GHZ\rangle = \exp(\frac{i\pi}{4}\sum_i X_i)\exp(\frac{i\pi}{8}\sum_{ij} Z_iZ_j)\exp(\frac{3i\pi}{4N}\sum_i X_i)\exp(\frac{i\pi}{4}\sum_{ij} Z_iZ_j)|+...+\rangle. \tag{23}$$

It is sufficient to establish

$$\langle\uparrow ...\uparrow|\exp(\frac{i\pi}{4}\sum_i X_i)\exp(\frac{i\pi}{8}\sum_{ij} Z_iZ_j)\exp(\frac{3i\pi}{4N}\sum_i X_i)\exp(\frac{i\pi}{4}\sum_{ij} Z_iZ_j)|+...+\rangle = \frac{1}{\sqrt{2}}, \tag{24}$$

up to a phase. (The Ising symmetry operator is conserved as $\prod X = 1$, so the matrix element for $\langle\downarrow ...\downarrow|$ will also be $\frac{1}{\sqrt{2}}$).

We break the matrix element in half and first the evaluate the left hand side. First,

$$\exp(\frac{-i\pi}{4}\sum_i X_i)|\uparrow ...\uparrow\rangle = \frac{1}{\sqrt{2^N}}\big(\prod_i(1-iX_i)\big)|\uparrow ...\uparrow\rangle \tag{25}$$

$$= \frac{1}{\sqrt{2^N}}\sum_s(-i)^{(N-\sum_i z_i)/2}|z\rangle, \tag{26}$$

where $z = \{z_1, ...z_N\}$ labels a spin configuration.

Applying $\exp(\frac{-i\pi}{8}\sum_{ij} Z_iZ_j)$ and neglecting overall phase then gives

$$\frac{1}{\sqrt{2^N}}\sum_z \exp(-i\pi/8\sum_{ij} z_iz_j)i^{\sum_i z_i/2}|z\rangle \tag{27}$$

$$= \frac{1}{\sqrt{2^N}}\sum_z \exp(\frac{i\pi}{16}(-z_t^2+4z_t))|z\rangle, \tag{28}$$

where we have defined $z_t \equiv \sum_i z_i$.

The right hand side is:

$$\exp(\frac{3i\pi}{4N}\sum_i X_i)\exp(\frac{i\pi}{4}\sum_{ij} Z_iZ_j)|+...+\rangle \tag{29}$$

$$= \frac{1}{\sqrt{2^N}}\exp(\frac{3i\pi}{4N}\sum_i X_i)\sum_z \exp(\frac{i\pi}{4}\sum_{ij} z_iz_j)|z\rangle \tag{30}$$

$$= \frac{1}{\sqrt{2^N}}\prod_i(c+isX_i)\sum_z \exp(\frac{i\pi}{4}\sum_{ij} z_iz_j)|z\rangle \tag{31}$$

where $c \equiv \cos(3\pi/4N), s \equiv \sin(3\pi/4N)$.

Consider the contributions to the coefficient of a given spin configuration $|z\rangle$. Each contribution involves partitioning the N spins into two sets A and B of sizes a and $N-a$ respectively, and flipping the spins in set A. The resulting coefficient from this given flip is

$$c^{N-a}(is)^a\exp(\frac{i\pi}{4}\sum_{ij} z_iz_j)\exp(\frac{i\pi}{4}\sum_{i\in A, j\in B}(\bar{z_i}-z_i)z_j), \tag{32}$$

where $\bar{z_i} \equiv -z_i$.

We now show that this factor only depends on the parity of a (and the particular configuration z) and once this is fixed, the factor is independent of the partition. The final phase factor above can be written as

$$\exp(\frac{-i\pi}{2}z_A(z_t-z_A)), \tag{33}$$

where $z_A \equiv \sum_{i\in A} z_i$. Because N is even, z_t is even. If a is even, the z_a is even and thus the phase factor is 1. Moreover, it is straightforward to check that either changing the partition (keeping partition size fixed) or changing

the partition size by 2 does not change the above phase. Hence, the case of a odd can be reduced to choosing A to be the first spin. The wavefunction becomes

$$\frac{1}{\sqrt{2^N}}\sum_z \exp(\frac{i\pi}{4}\sum_{ij} z_i z_j)\Big(\sum_{\text{even } a}\binom{N}{a}c^{N-a}(is)^a + \sum_{\text{odd } a}\binom{N}{a}c^{N-a}(is)^a \exp(\frac{-i\pi}{2}z_1(z_t-z_1))\Big)|z\rangle$$
$$= \frac{1}{\sqrt{2^N}}\sum_z \exp(\frac{i\pi}{4}\sum_{ij} z_i z_j)\Big(\cos(3\pi/4) + i\sin(3\pi/4)\exp(\frac{-i\pi}{2}z_1(z_t-z_1))\Big)|z\rangle$$

Dropping overall phases, we get

$$\frac{1}{\sqrt{2^{N+1}}}\sum_z \exp(\frac{i\pi}{8}z_t^2)\Big(1 - i\exp(\frac{-i\pi}{2}z_1(z_t-z_1))\Big)|z\rangle \tag{34}$$

The matrix element between left and right hand sides is thus

$$\frac{1}{2^N\sqrt{2}}\sum_z \exp(\frac{i\pi}{16}(3z_t^2-4z_t))(1 - i\exp(\frac{-i\pi}{2}z_1(z_t-z_1)) \tag{35}$$

Due to the last piece, any configuration with $z_t \equiv 2(\text{mod } 4)$ does not contribute and the matrix element reduces to

$$\frac{1}{2^N\sqrt{2}}\sum_{z|z_t\equiv 0(\text{mod } 4)} 2\exp(\frac{i\pi}{16}(3z_t^2-4z_t)) \tag{36}$$
$$= \frac{1}{\sqrt{2}}. \tag{37}$$